

Synthesis and characterization of fluorene-derived PU as a thermo cross-linked hole-transporting layer for PLED

Ching-Nan Chuang^a, Chao-Hui Kuo^a, Yu-Shan Cheng^a, Chih-Kai Huang^a, Man-kit Leung^{a,c,*}, Kuo-Huang Hsieh^{a,b,*}

^a Institute of Polymer Science and Engineering, National Taiwan University, Taipei 106, Taiwan

^b Department of Chemical Engineering, National Taiwan University, Taipei 106, Taiwan

^c Department of Chemistry, National Taiwan University, Taipei 106, Taiwan

ARTICLE INFO

Article history:

Received 19 December 2011

Received in revised form

5 March 2012

Accepted 8 March 2012

Available online 15 March 2012

Keywords:

PLED

Polyurethane

Hole-transporting material

ABSTRACT

Novel hole-transporting polyurethane, denoted as **P1**, resulting from the condensation of 9, 9-bis(4-hydroxyphenyl)fluorene and isophorone diisocyanate (denoted as IPDI) has been developed. When **P1** is thermally consolidated in the presence of 2-(phosphonoxy)ethyl methacrylate (**P2M**), it forms a distinguished hole-transport layer that leads to an extremely good performance of the phosphorescent PLED. In the study, the device of ITO/PEDOT: PSS/**P1-P2M**/Ir(ppy)₃-t-PBD-PVK/Mg/Ag shows a high current efficiency of 27.6 cd/A and a low turn-on voltage of 6 V. In particular, the stable output efficiency of 17–22 cd/A within the range of 420–4400 cd/m² at 12–20 V makes **P1** a promising hole-transport material for phosphorescent PLED applications.

© 2012 Elsevier Ltd. All rights reserved.

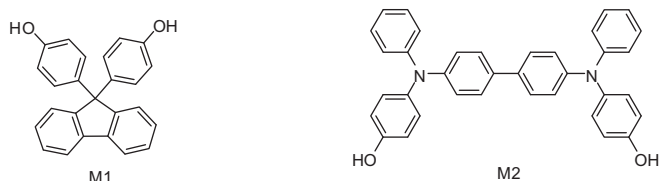
1. Introduction

Organic electronic polymers have attracted considerable interest because of their applications in polymer light-emitting diodes (PLEDs) [1–5], organic thin-film transistors (OTFTs) [6–8], flexible flat-panel display [9] and photovoltaic cells [10,11]. Among the classes of electroluminescent (EL) conjugated polymers, poly(*p*-phenylenevinylene)s (PPVs) [12] and poly(9,9-dialkylfluorene)s (PFs) [13] are two families that have attracted a lot of attention during the past decade. PFs and their derivatives are promising blue-light-emitting materials that are widely used in PLEDs due to their excellent thermal and chemical stability, as well as their high photoluminescence (PL) quantum yield [14–17] and π -electron excessive (electron-rich) in nature and hence have better hole-injection and hole-transporting ability [18–21]. However, the mismatched HOMO energy level of 5.8 eV [22,23] builds up a high hole-injection barrier, and an unbalance charge injection could lead to poor performance of the organic electronic devices. To solve this problem, there are two strategies have been adopted, one is through appropriate design of chemical structure and the other is

optimized of the device structure. For the first strategy, the incorporation of hole-transporting moieties on a main or side chain, such as triphenylamine, is usually adopted to improve hole-injection from anode [24,25]. For the second strategy, multilayer devices are required and fabricated by adding an extra hole-transporting layer (HTL), such as poly(styrenesulphonate):poly(3,4-ethylenedioxythiophene) (PEDOT: PSS), to reduce the hole-injection barrier from anode [26,27]. An ideal device should have a smooth charge carrier injection, and balanced charge transport properties in the polymer layer. The presence of a high injection barrier usually results in a high driving voltage, which leads to an increased thermal loading for the polymer layer; therefore, a good hole-transporting layer (HTL) plays a very important role in fabricating a high efficiency multilayer PLED. It bridges the hole-injection from an indium tin oxide (ITO) anode into a light-emitting layer (EML), which results in balanced charge-injection/transport and better device performance. Material to be used as an efficient HTL in multilayer PLEDs has to possess very good solvent resistance for multilayer processing. To achieve this purpose, either photo- or thermally cross-linked hole-transporting materials or a suitable solvent combination are usually employed to consolidate the bottom layer [28–37]. Recently, Wong reported that fluorene derivatives show good charge transport behavior [38,39]. Certain challenges are posed, however, for carrier-transport properties that are both fundamental and practical interest, because linear conjugated polymers in films generally have a strong tendency to form crystalline domains. Although sporadic reports exist on carrier-transport

* Corresponding authors. Institute of Polymer Science and Engineering, National Taiwan University, Taipei 106, Taiwan. Tel.: +886 2 33663044; fax: +886 2 33661673.

E-mail addresses: mkleung@ntu.edu.tw (M.-k. Leung), khhsieh@ntu.edu.tw (K.-H. Hsieh).



Scheme 1. Structure of **M1** and **M2**.

properties as a function of polymer lengths in crystalline states of some conjugated polymers, such as polythiophenes and polyacenes [40–44], however, they give no representation of the generally amorphous (disordered) situation in polymer films. To obtain a truly amorphous film to study, diaryl substituents have been introduced at the C9 of fluorene, leading to enhanced morphological stability of the amorphous phase and exhibiting intriguing non-dispersive ambipolar carrier-transport properties. The other method was to isolate the function group, such as ether linkage, silane, alkyl chain, urethane, etc. The usage of this kind of linkage realizes an unlimited mixing of active side groups and causes a stable morphology, since both migration and aggregation are significantly suppressed by fixing the active molecules as side groups [45,46].

Polyurethanes (PUs) are common polymers that are widely used in industrial applications due to their properties: elasticity, flexibility, thermal stability, and excellent chemical resistance [47–52]. Several studies on the applications of PUs on PLEDs have recently been reported [53–57]. In our previous reports [36,47,54,55], we demonstrated that polymers with urethane linkages enhance hole-injection performance between PEDOT: PSS and EML.

In this work, two series of polyurethanes were synthesized and characterized: the first series comprised the homopolymers of fluorene type polyurethane (**P1**) and triphenylamine type polyurethane (**P5**). The second series comprised the copolymers of triphenylamine-co-9, 9-bis(4-hydroxyphenyl)fluorene derivatives (**P2–P4**) [58–62]. PUs were ideal candidates in our study due to their metal-ion-free synthetic pathway. A low level of metal-ion contaminants is an essential requirement for high performance electronic polymers. PUs were prepared from condensation of diols and diisocyanates, in which no metal-ion-containing reagents were involved so that metal-ion contaminations could be avoided.

2. Experimental

2.1. Materials

N, *N'*-bis(4-hydroxyphenyl)-*N*, *N'*-diphenylbenzidine was prepared in our previous work [55]. Reagent grade chemicals and solvents were purchased from Aldrich, ACROS, Fluka, and Lancaster Chemical Co. THF, dichloromethane and DMF were dried over sodium/benzophenone, P_2O_5 and calcium hydride respectively and

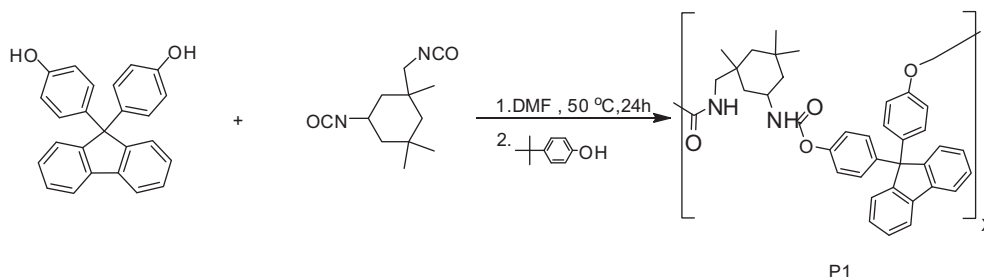
freshly distilled before use. Tetrabutylammonium perchlorate (TBAP) was recrystallized twice from ethyl acetate and vacuum-dried for two additional days. The other chemicals were used without further purification. The chemical structures for all of the products were confirmed by 1H NMR spectroscopy, mass spectra (FAB) and elemental analyses.

2.2. Characterization methods

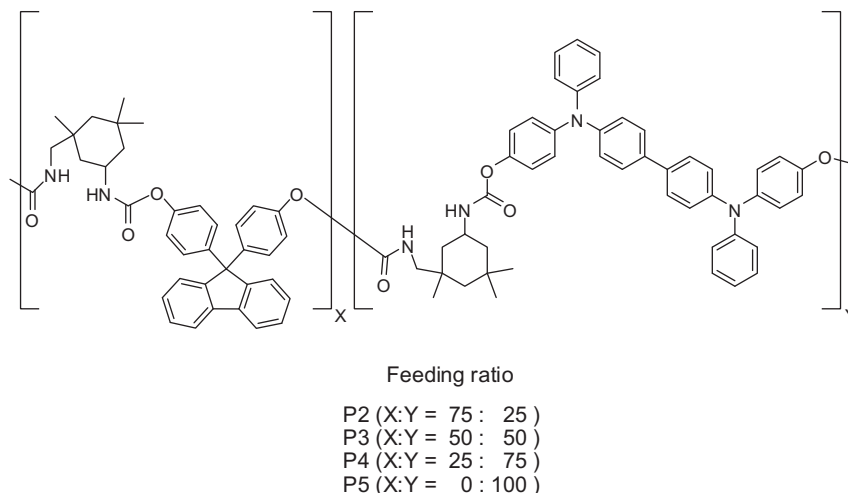
1H NMR spectra were measured on a Bruker 400 MHz spectrometer. Elemental analyses were measured using an EA Heraeus Vario EL-3 analyzer. FT-IR spectra were recorded on a Jasco-480 spectrometer. UV–Vis analyses were obtained from a Jasco V-570 UV–Vis spectrophotometer. The number-average and weight-average molecular weight of the polymers were determined by a Waters GPC-480 system with a column of AM GPC Gel (10 μm) from the American Polymer Standard Company. Dimethylformamide (DMF) was used as eluent and polystyrene as the standard in the GPC experiments. TGA and DSC were performed on a TGA Perkin–Elmer TGA-7 and a DSC Du Pont 2010 analyzer under nitrogen atmospheric conditions at a heating rate of 10 $^{\circ}C\ min^{-1}$. The thickness of the polymer films was measured using an Alpha step Dektak 3030 profilometer. PL spectra of the polymers were recorded using a Hitachi-4500 spectrofluorometer. Cyclic voltammetric measurements of the material were made in DMF with 0.1 M tetrabutylammonium perchlorate (TBAP) as the supporting electrolyte at a scan rate of 100 mV/s. Platinum wires were used as both the counter and working electrodes, and silver/silver ions (Ag in 0.1 M AgCl solution) was used as the reference electrode. Ferrocene was used as an internal standard, and the potential values were obtained and converted to vs. SCE (saturated calomel electrode) [63]. Electroluminescence was recorded on a Minolta CS-100A instrument. The *I*–*V* and *L*–*V* characteristics of the devices were measured by integrating a Keithley 2400 source-meter as the voltage and current source and a Minolta CS-100A instrument as the Luminance detector. All of the measurements and device fabrications were performed at room temperature in a dust-controlled environment.

2.3. Device fabrication

Two kinds of device structures were adopted in this study. The first type of device was fabricated with ITO/PEDOT: PSS/PUs/Ir(ppy)₃ + PVK+*t*-PBD/Mg/Ag where there was no thermal cross-linked agent contained in the PUs layer. The second device contained a cross-linked agent [2-(phosphonooxy)ethyl methacrylate (**P2M**)] in the PU layer which was thermally cross-linked prior to metal vapor deposition. The ITO surface was cleaned by sonication, and rinsed sequentially in de-ionized water, Triton-100 water solution, de-ionized water, acetone, and methanol. For the previous structure, the hole-injection material: PEDOT: PSS was spin-coated



Scheme 2. PUs synthetic route of the fluorene type (**P1**).



Scheme 3. PUs structure of copolymers: **P2–P5**.

at 5000 rpm, 60 s, on top of the ITO glass and dried on a hot plate at 130 °C for 30 min within a vacuum. The PU solution was spin-coated at 4000 rpm, 60 s, onto the prepared ITO/PEDOT-PSS anode and dried under reduced pressure for 30 min at 120 °C; it contained 2.5% **P2M** of PU which was spin-coated at 4000 rpm, 60 s and dried under reduced pressure for 30 min at 150 °C in order to form cross-linkable film. The emitting layer solution of concentration of Ir(ppy)₃ (4 mg) + PVK(50 mg) + *t*-PBD(20 mg)/in chloroform(4 mL) was spin-coated at 3000 rpm, 90 s, on the surface of ITO/PEDOT: PSS/PU. The Mg and Ag contacts were deposited on ITO/PEDOT-PSS/PU/EML at pressure below 10^{−6} torr. The deposition rates of Mg and Ag cathodes were 1.0 Å/s and 4.0 Å/s, giving an active area of 0.125 cm².

2.4. Monomer synthesis

9,9-Bis(4-hydroxyphenyl)fluorene (**M1**) was prepared from the condensation of 9-fluorenone and phenol using cationic ion-exchange resins as catalysts in 83% yields [64–67]. **M2** was synthesized as described in our previous literature [55]. Scheme 1 is the structure of **M1** and **M2**.

2.5. Synthesis of fluorene type polyurethane as hole-transporting layer **P1** to **P5**

The general synthetic procedures for the polymers are described as follows [54,55]:

P1 and **P5**: 9, 9-Bis(4-hydroxyphenyl)fluorene (5 mmol) or *N,N'*-bis(4-hydroxyphenyl)-*N,N'*-diphenylbenzidine (5 mmol),

isophorone diisocyanate (IPDI, 5.25 mmol) and dried DMF (25 mL) were charged in a two-necked flask, and stirred for 24 h at 50 °C under nitrogen. 4-*tert*-Butylphenol (0.5 mL) was added and stirred for 24 h to terminate the reaction. When the reaction was complete, the reaction mixture was poured into methanol and the desired PU would precipitate. The PU was then collected and purified by dissolving in DMF and reprecipitated from methanol several times. The synthesis process is illustrated in Scheme 2. The polymers were characterized by ¹H NMR and FT-IR.

P1: Anal. Calcd: C, 76.86; H, 6.64; N, 5.63%. Found: C, 75.94; H, 7.24; N, 5.03%. ¹H NMR (400 MHz in DMSO-*d*₆): δ 7.90–7.88 (m, 2H), 7.40–6.98 (m, 8H), 6.64–6.62 (m, 2H), 1.52–1.26 (m, 6H), 1–0.87 (m, 9H), IR(KBr): 3318, 1725, 1600, 1450, 820.

P5: Anal. Calcd: C, 74.1; H, 6.60; N, 9.0%. Found: C, 73.9; H, 6.84; N, 8.8%. ¹H NMR (400 MHz, DMSO-*d*₆): δ 7.6–7.4 (m, 4H), 7.3–7.2 (m, 4H), 7.1–6.9 (m, 18H), 3.7–3.6 (m, 4H), 1.2–0.7 (m, 15H), IR (KBr): 3321, 1725, 1600, 1450, 820.

P2, P3 and **P4**: 9, 9-Bis(4-hydroxyphenyl)fluorene and *N,N'*-bis(4-hydroxyphenyl)-*N,N'*-diphenylbenzidine with the feeding ratio of 3:1, 1:1 and 1:3, IPDI and dried DMF were charged in a two-necked flask, and stirred for 24 h at 50 °C under nitrogen. 4-*tert*-Butylphenol was added and stirred for 24 h to terminate the reaction. When the reaction was complete, the reaction mixture

Table 1
Average molecular weights and thermal properties of PUs: **P1–P5**.

Polymer	<i>M_w</i> ^a	<i>M_n</i>	PDI	<i>T_g</i> (°C) ^c	<i>T_d</i> (°C) ^b
P1	7900	5900	1.33	165	274
P2	5000	3500	1.43	173	296
P3	6300	4500	1.40	175	290
P4	7600	7200	1.05	176	282
P5	7500	4000	1.87	174	274

^a Determined by GPC by eluting with DMF, by comparison with polystyrene standards.

^b Temperature at which a 5% weight loss occurred was determined at a heating rate of 10 °C/min under a nitrogen atmosphere.

^c The value of *T_g* was determined at a heating rate of 10 °C/min under a nitrogen atmosphere.

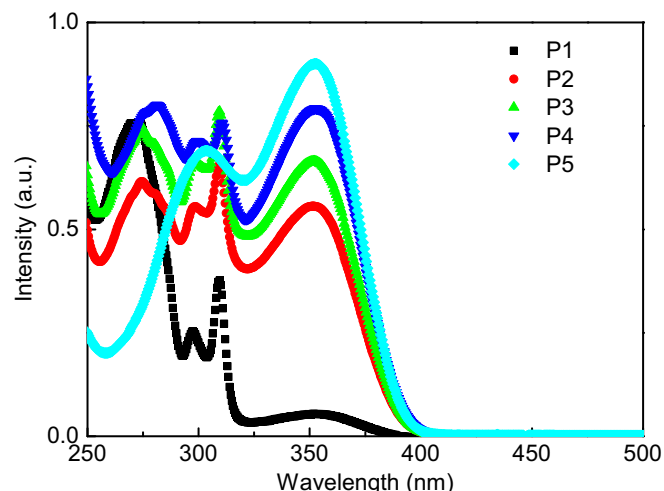


Fig. 1. UV–Vis absorption spectra of **P1–P5** in DMF solution.

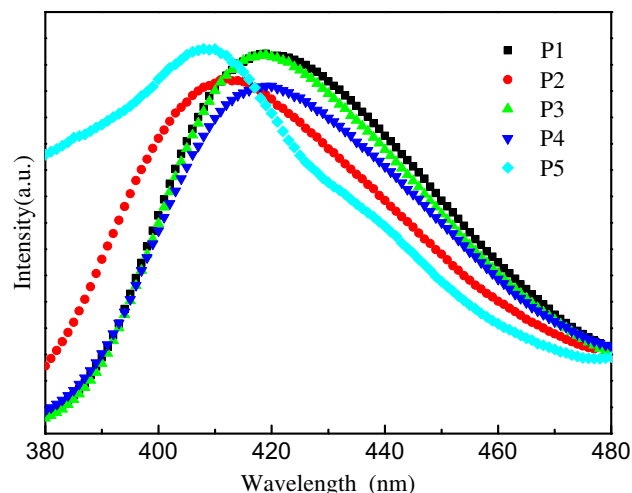


Fig. 2. PL spectra of P1–P5 in a solid film.

Table 2
Optical properties of PUs: P1–P5.

Polymer	UV–Vis λ_{\max} solution ^a (nm)	PL λ_{\max} solution ^b (nm)	Optical E_{gap} (eV)	HOMO (eV)	LUMO (eV)
P1	281(272) ^c	410(408) ^d	3.19	5.33	2.14
P2	318(308)	410(419)	3.10	5.25	2.15
P3	318(308)	413(418)	3.17	5.12	1.95
P4	320(309)	409(413)	3.13	5.26	2.13
P5	315(305)	414(420)	3.10	5.30	2.20

^a Concentration: 1×10^{-5} M in DMF.

^b Concentration: 1×10^{-6} M in DMF.

^c The value in parentheses represents the value of $\lambda_{\text{absmax}}(\text{nm})$ of the polymer as a solid film.

^d The value in parentheses represents the value of $\lambda_{\text{PLmax}}(\text{nm})$ of the polymer as a solid film.

was poured into methanol and the desired PUs would precipitate. The PUs were collected and purified by dissolving in DMF and reprecipitated from methanol and toluene for several times in order to remove any oligomeric residue. Scheme 3 is the PU structure of the copolymer P2–P5. The polymers were characterized by ¹H NMR and FT-IR.

P2: Anal. Calcd: C, 74.59; H, 6.44; N, 7.74%. Found: C, 75.79; H, 6.76; N, 7.79%. ¹H NMR (400 MHz in DMSO-*d*₆): δ 7.96–7.88 (m, 16H), 7.37–7.18 (m, 17H), 6.97–6.6 (m, 15H), 1.52–1.22 (m, 12H), 1.3–0.7 (m, 18H), IR (KBr): 3318, 1725, 1600, 1450, 820.

P3: Anal. Calcd: C, 74.39; H, 6.55; N, 7.5%. Found: C, 74.59; H, 6.78; N, 7.37%. ¹H NMR (400 MHz in DMSO-*d*₆): δ 7.96–7.88 (m, 16H), 7.37–7.18 (m, 17H), 6.97–6.6 (m, 15H), 1.52–1.22 (m, 12H), 1.3–0.7 (m, 18H), IR (KBr): 3324, 1725, 1600, 1450, 820.

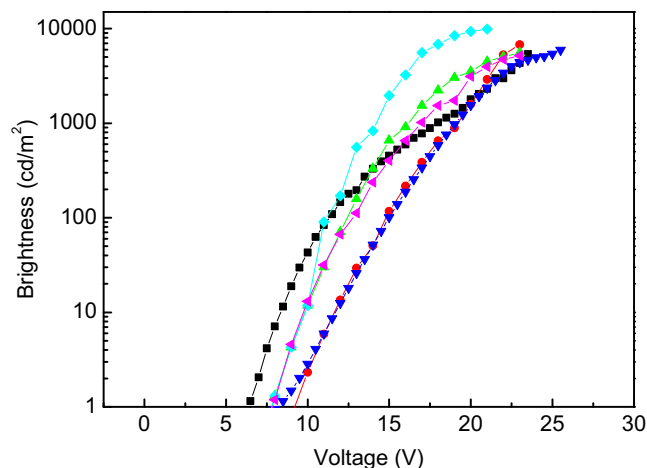


Fig. 4. The B–V of the P1–P5 in DP1 to DP5 including standard device STD: ■ – DP1, ● – DP2, ▲ – DP3, ▼ – DP4, ◆ – DP5, ▲ – STD.

P4: Anal. Calcd: C, 74.39; H, 6.65; N, 7.25%. Found: C, 75.13; H, 6.8; N, 7.1%. ¹H NMR (400 MHz in DMSO-*d*₆): δ 7.96–7.88 (m, 16H), 7.37–7.18 (m, 17H), 6.96–6.6 (m, 15H), 1.7–1.4 (m, 12H), 1.27–0.7 (m, 18H), IR (KBr): 3324, 1725, 1600, 1450, 820.

3. Results and discussion

3.1. Synthesis and characterization

The condensation polymerization of the polyurethane in dried DMF were synthesized with commercially available IPDI as the non-conjugated linkages incorporation of 9,9-bis(4-hydroxyphenyl)fluorene (**M1**) and *N,N'*-bis(4-hydroxyphenyl)-*N,N'*-diphenylbenzidine (**M2**), with feeding ratios of 1:0, 3:1, 1:1, 1:3 and 0:1 being introduced. The molecular weight data of the prepared PUs including M_n , M_w , PDI value were determined by gel-permeation chromatography (GPC) analysis against polystyrene standard in DMF. In addition, the GPC results and their thermal properties, including T_g and T_d were listed in Table 1. It can be seen that the M_n and M_w values of these PUs are in the range of 3500–7200 and from 5000 to 7900, respectively, with PDI less than 1.87.

3.2. Thermal properties

The thermal behavior of the P1–P5 was measured by thermogravimetric analysis (TGA) and differential scanning calorimetry (DSC). The thermal decomposition temperatures (T_d , 5% weight loss) and the glass transition temperatures (T_g) of five PUs are also listed in Table 1. All polymers showed high T_g 's above 160 °C and

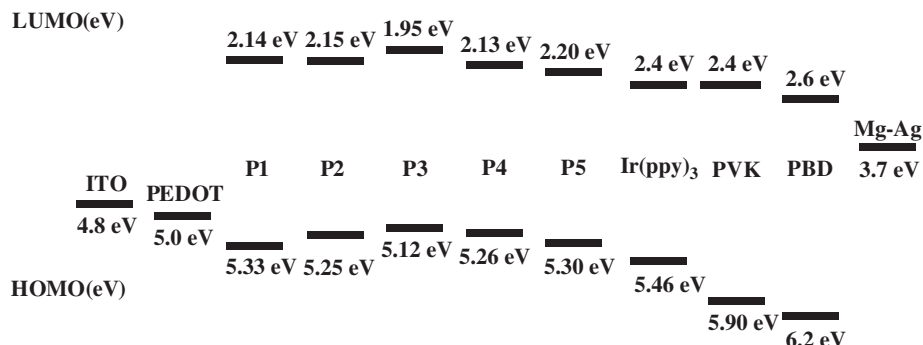


Fig. 3. Energy level diagram of the ITO/PEDOT: PSS/P1–P5/EML/Mg/Ag device.

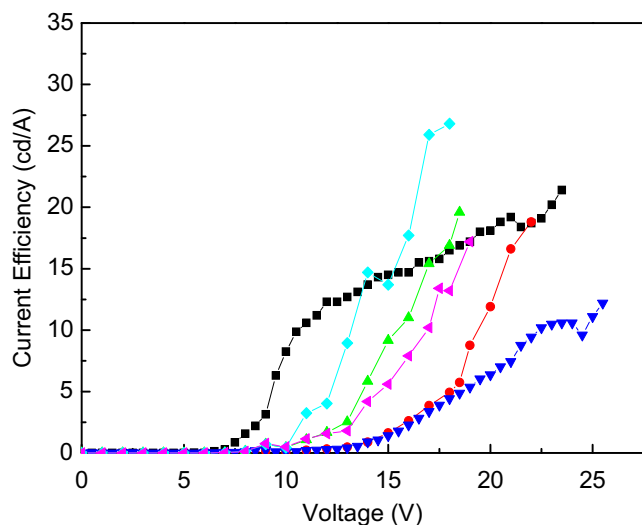


Fig. 5. The current efficiency of **P1–P5** in DP1 to DP5 including standard device STD: \blacksquare - DP1, \bullet - DP2, \blacktriangle - DP3, \blacktriangledown - DP4, \blacklozenge - DP5, \blacktriangleleft - STD.

T_d 's above 274 °C. The high thermal resistance of the polymers would be beneficial for the device fabrication, against the high temperature conditions during the thermal vapor deposition of the metallic cathode. Thermal stability of the polymer is an important factor for PLED application. The thermal properties were highly related to the performance as well as the lifetime of the devices. Materials having too low of T_g and T_d may decompose or cause morphological change, deformation and degradation under operating conditions and thus create obstacles in transporting holes and electrons in the device, hampering the device performance [49,50].

3.3. Optical properties

The optical properties of **P1–P5** were measured both in solution and in solid thin-film. Transparent uniform films of **P1–P5** were prepared on a quartz substrate by spin-coating DMF solutions. Their spectra are shown in Figs. 1 and 2. Table 2 summarizes their absorption maxima. Homopolymer **P1** (only fluorene type) shows that absorption peaked at 272 nm. **P2–P5** exhibited an additional absorption band peaking in the region of 350 nm, which were assigned to π - π^* electronic transition of the triphenylamine group. No spectral wavelength shift in their solution spectra was observed, indicating that the intra-chain between triphenylamine and fluorene was minimal. The triphenylamine absorption reduced along with a decrease in the **M2** content, which is consistent with their feed ratios. The photoluminescence (PL) spectra of **P1–P5** in solid film are illustrated in Fig. 2. Their fluorescence peaked around 420 nm and exhibited similar band widths.

Table 3
Devices performances of the **P1–P5** in system (1).

Device	Turn-on voltage at 1 cd/m ² (V)	Max. brightness (cd/m ²)/voltage (V)	Efficiency (cd/A)/voltage (v)
DP1	6.5	5390/21.5	21.4/23.5
DP2	9	6800/23	18.8/22
DP3	8	5540/23	19.6/18.5
DP4	8.5	5950/25.5	12.2/25.5
DP5	7.5	9910/21	26.8/18
STD	8	5190/23	17.2/19

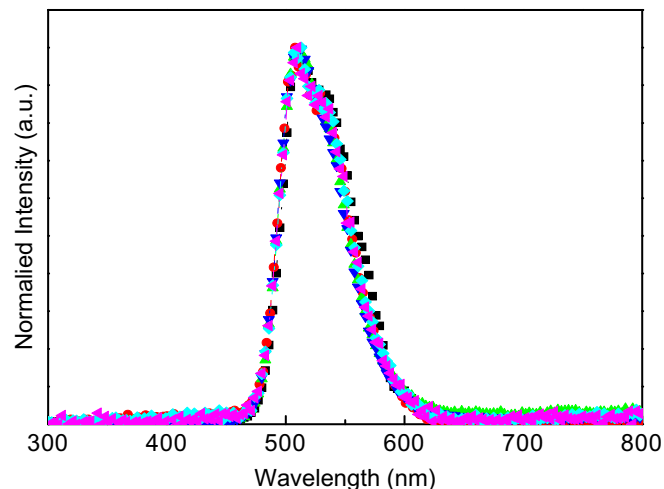


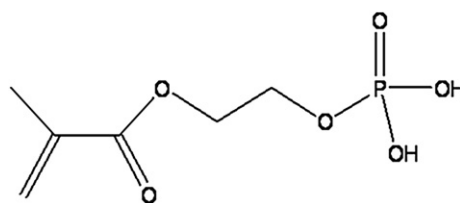
Fig. 6. The electroluminescence spectra of **P1–P5** in DP1 to DP5 including standard device STD: \blacksquare - DP1, \bullet - DP2, \blacktriangle - DP3, \blacktriangledown - DP4, \blacklozenge - DP5, \blacktriangleleft - STD.

3.4. Electrochemical properties

Cyclic voltammetry measurements have previously been demonstrated to investigate the energy levels of the three polymers. When the applied potential reached the oxidation (reduction) potential, the redox reaction took place on the surface of the electrode and redox current occurred. This critical potential is termed “onset potential”. The onset potential was determined by the obvious turning of the curve observed in the CV diagram. The corresponding highest occupied molecular orbital (HOMO) was estimated with standard ferrocene potential at 4.8 eV. The estimated values of **P1–P5** are shown in Table 2. E_g was determined by the equation $1240/\lambda_{\text{onset(nm)}}$ [68,69], where the λ_{onset} was referred to as the value of onset absorption wavelength. The lowest-unoccupied molecular orbital (LUMO) energy levels were then estimated according to the following equation: $E_{\text{LUMO}} = E_{\text{HOMO}} - E_g$. According to the above analysis, the HOMO values of all these polymers were found to be between 5.12 and 5.33. This result indicates that these are potentially good hole-transport materials for PLED devices. On the other hand, the LUMO values of these polymers were found to be between 1.95 and 2.20. The optical range gap of all these polyurethanes are within the range of 3.10–3.19 eV and the energy level of the device was therefore constructed, as shown in Fig. 3.

3.5. Electroluminescence properties

The first series of [ITO/PEDOT: PSS (30 nm)/PU (30 nm)/Ir(ppy)₃ + PVK+t-PBD (65 nm)/Mg (2 nm)/Ag (100 nm)] PLEDs were fabricated, using the successive layer-by-layer spin-coating approach to establish a multilayer structure. Although the apparent electroluminescence performance of this series looked



Scheme 4. Structure of cross-linking agent **P2M**.

Table 4
Device performance of **P1–P5** in system (2).

Device	Turn-on voltage (V) at 1 cd/m ²	Max. brightness (cd/m ²)/voltage (V)	Max. efficiency (cd/A)/voltage (V)
DDP1	6	9560/21.5	27.6/21.5
DDP2	9	8560/24.5	18/24.5
DDP3	8.5	7290/23.5	16.5/23.5
DDP4	9	7920/25	16.2/25
DDP5	7.5	9530/19	27/19
STD	8	5190/23	17.2/19

*Operational lifetime of DDP1 was compared with DP1 and STD (see [Supplementary information](#)).

attractive, the device performance was relatively irregular. The maximum luminescence obtained for DP1–DP5 respectively was 5390, 6800, 5540, 5950 and 9910 cd/m², with maximum current efficiency of 21.4, 18.8, 19.6, 12.2 and 26.8 cd/A, as illustrated in Figs. 4 and 5. The brightness-voltage and current efficiency-voltage results of the devices are summarized in Table 3. Since the PU layer had not been thermally cross-linked during the layer-by-layer spin-coating process, we suspected that a swelling or partial re-dissolution of the PU film would occur during spin-coating of the light-emitting layer, causing an irregularity in the performances of the devices. The electroluminescence spectra of DP1–DP5 and STD are shown in Fig. 6. The EL spectra illustrates that the maximum emission peak locates at the 510 nm wavelength. This indicates the hole-transport PU layer inserted between PEDOT: PSS and EML wouldn't affect the EML emission.

However, it is noteworthy to point out that the turn-on voltage for the device of DP1 was particularly low. In our study, the turn-on voltage was reduced down to 6.5 V, which is about 1.5 V lower than that of the STD device (8V). The efficiency was up to 21.4 cd/A which was higher than that of 17.2 cd/A for the STD device. More interesting is the stable output efficiency between voltages of 10 V and 20 V, corresponded to the EL output range of 100–4000 cd/m². The unexpectedly good outcomes from the DP1 device encouraged us to further explore any possibilities to improve the construction of the device.

To solve the problem of the partial re-dissolution of PU film during the layer-by-layer spin-coating process, the PU layer was blended with 2-(phosphonooxy)ethyl methacrylate (**P2M**, 2.5 wt%, as shown in Scheme 4) as a cross-linking agent. The layer was thermally treated at 150 °C for 30 min to induce cross-linking before the light-emitting layer was spin-coated on top. The

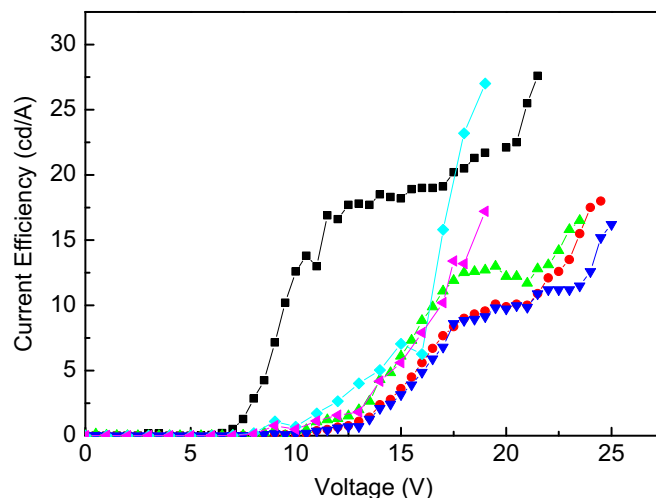


Fig. 8. The current efficiency of **P1–P5** in DDP1 to DDP5 including standard device STD: -■- DDP1, -●- DDP2, -▲- DDP3, -▼- DDP4, -◆- DDP5, -◄- STD.

presence of the phosphate group on **P2M** helped the cross-linking agent to be doped into the PEDOT: PSS layer, thereby improving the surface contact between the PEDOT: PSS and the PU layers.

Table 4 summarizes the brightness and current efficiency of the DDP1–DDP3 devices. The results are also illustrated in Figs. 7 and 8 respectively. Luminescence levels of up to 9560, 8560, 7290, 7920 and 9530 cd/m² were recorded for devices DDP1–DDP5. The maximum current efficiency of the devices are 27.6, 18, 16.5, 16.2 and 27 cd/A, under operating voltages of: 21.5, 24.5, 23.5, 25 and 19 V, respectively. It is noteworthy to point out while the performance of DDP2–DDP5 were similar, as shown in Figs. 7 and 8, the performance of DDP1 stood out from the others. The DDP1 device exhibited significant improvement in current efficiency (27.6 cd/A), higher than STD by 17.2 cd/A, with a turn-on voltage drop to 6 V. Particularly, the low turn-on voltage of 6 V and the stable output efficiency of 17–22 cd/A within the range of 420–4400 cd/m² at 12–20 V suggested that **P1** was an extremely effective hole-transport material. On the other hand, the performance of the **M2** containing polymers was relatively poor, in comparison to that of **P1**. It is probably due to the electron-rich structure of **M2** which can form very stable radical cations after oxidation and therefore possibly hamper the hole-mobility of the polymer matrix. In

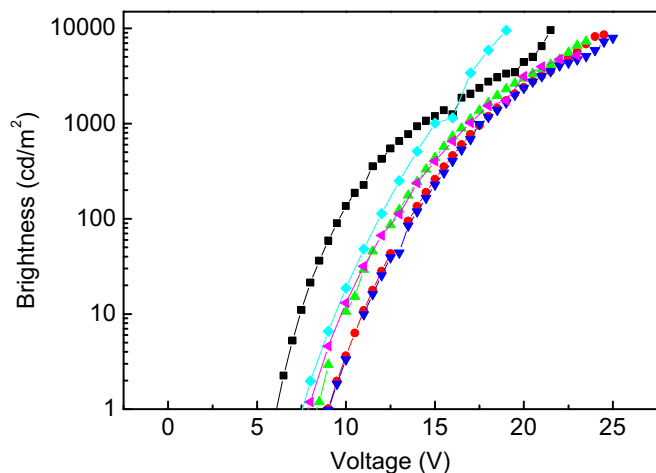


Fig. 7. The B–V of the **P1–P5** in DDP1 to DDP5 including standard device STD: -■- DDP1, -●- DDP2, -▲- DDP3, -▼- DDP4, -◆- DDP5, -◄- STD.

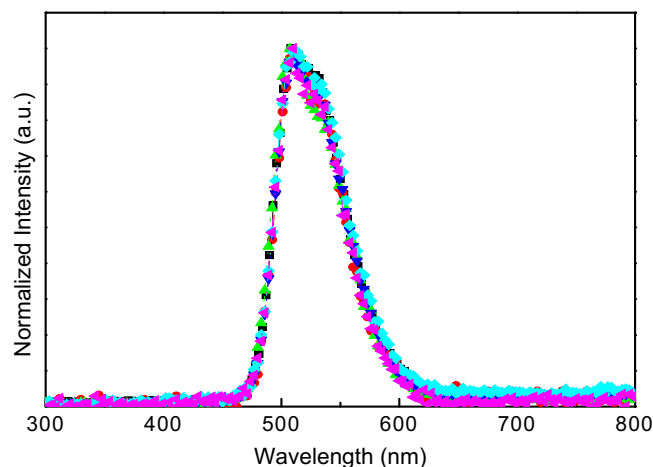


Fig. 9. The electroluminescence spectra of **P1–P5** in DDP1 to DDP5 including standard device STD: -■- DDP1, -●- DDP2, -▲- DDP3, -▼- DDP4, -◆- DDP5, -◄- STD.

addition, the stable benzidine cationic structure of each **M2** fragment is known to be colored and have a low NIR optical gap, corresponding to intervalence charge-transfer absorption, which might then lead to a partial quenching of the excitons in the matrix. The electroluminescence spectra of DDP1-DDP5 and STD are shown in Fig. 9. The EL spectra illustrates that the maximum emission peak were similar the DP1-DP5 devices. This indicates the cross-linked hole-transport PU layer wouldn't affect the EML emission.

4. Conclusion

We discovered that the fluorene type PU polymer, denoted as **P1**, exhibits outstanding performance as a novel hole-transporting materials. When **P1** is thermally consolidated in **P2M** present in the PLED, it forms a highly stable hole-transport layer. Consequently the PLED shows a low turn-on voltage of 6.0 V, and has a stable output efficiency of 17–22 cd/A within the range of 420–4400 cd/m². This is a very important breakthrough because materials having low triplet energy levels usually act as a triplet quencher and lead to poor device performance. Unfortunately, most of the conjugated aromatic compounds developed for PLED have similar difficulties. The present discovery provides us with a breakthrough for designing novel hole-transport materials for the phosphorescence-based PLED.

Acknowledgments

This work was supported by the Ministry of Economic Affairs (grant no. 96-EC-17-A-08-S1-015), the National Science Council of Taiwan (NSC 97-2221-E-002-025-MY3 and NSC 98-2119-M-002-006-MY3), and the Advanced Polymer Nano-technology Research Center (APNRC) of National Taiwan University.

Appendix A. Supplementary data

Supplementary data related to this article can be found online at doi:10.1016/j.polymer.2012.03.023.

References

- [1] Wang KL, Leung MK, Hsieh LG, Chang CC, Lee KR, Wud CL, et al. *Org Electronics* 2011;12(6):1048–62.
- [2] Shakutsui M, Matsuura H, Fujita K. *Org Electronics* 2009;10(5):834–42.
- [3] Kulkarni AP, Tonzola CJ, Babel A, Jenekhe SA. *Chem Mater* 2004;16(23):4556–73.
- [4] Mitschke U, Bäurele PJ. *J Mater Chem* 2000;10(7):1471–507.
- [5] Akcelrud L. *Prog Polym Sci* 2003;28(6):875–962.
- [6] Chen Z, Fang J, Gao F, Brenner TJK, Banger KK, Wang X, et al. *Org Electronics* 2011;12(3):461–71.
- [7] Tseng SR, Li SY, Meng HF, Yu YH, Yang CM, Liao HH, et al. *Org Electronics* 2008;9(3):279–84.
- [8] Chang JW, Liang PW, Lin MW, Guo TF, Wen TC, Hsu YJ. *Org Electronics* 2011;12(3):509–15.
- [9] Hong Y, Kanicki J. *IEEE Trans Electron Devices* 2004;51(10):1562–9.
- [10] Bundgaard E, Krebs FC. *Sol Energy Mater Sol Cells* 2007;91(11):954–85.
- [11] Leeuw DMD, Simenon MMJ, Brown AB, Einerhand REF. *Synth Met* 1997;87(1):53–9.
- [12] Chellappan V, Almantas P, Huang C, Chen Z, Ronald Ö, Chua SJ. *Org Electronics* 2007;8(1):8–13.
- [13] Kameshima H, Nemoto N, Endo T. *J Polym Sci Part A Polym Chem* 2001;39(18):3143–50.
- [14] Bernius MT, Inbasekaran M, O'Brien J, Wu W. *Adv Mater* 2000;12(23):1737–50.
- [15] Scherf U, List EJW. *Adv Mater* 2002;14(7):477–87.
- [16] Neher D. *Macromol Rapid Commun* 2001;22(17):1365–85.
- [17] Wu Z, Fan B, Li A, Xue F. *Org Electronics* 2011;12(6):993–1002.
- [18] Strukelj M, Papadimitrakopoulos F, Miller TM, Rothberg LJ. *Science* 1995;267(5206):1969–72.
- [19] Tonzola CJ, Alam MM, Jenekhe SA. *Adv Mater* 2002;14(15):1086–90.
- [20] Chen JC, Wu HC, Chiang CJ, Peng LC, Chen T, Xing L, et al. *Polymer* 2011;52(26):6011–9.
- [21] Hughes G, Bryce MR. *J Mater Chem* 2005;15(1):94–107.
- [22] Janietz S, Bradley DDC, Grell M, Giebeler C, Inbasekaran M, Woo EP. *Appl Phys Lett* 1998;73(5):2453–5.
- [23] Babel A, Jenekhe SA. *Macromolecules* 2003;36(20):7759–64.
- [24] Ma W, Iyer PK, Gong X, Liu B, Moses D, Bazan GC, et al. *Adv Mater* 2005;17(3):274–7.
- [25] Su WF, Chen Y. *Polymer* 2011;52(15):3311–7.
- [26] Lim B, Hwang JT, Kim JY, Ghim J, Vak D, Noh YY, et al. *Org Lett* 2006;8(21):4703–6.
- [27] Liu MS, Niu YH, Ka JW, Yip H-L, Huang F, Luo J, et al. *Macromolecules* 2008;41(24):9570–80.
- [28] Parker D, Pei Q, Marrocco M. *Appl Phys Lett* 1994;65(10):1272–4.
- [29] Gruener JH, Wittmann F, Hamer PJ, Friend RH, Huber J, Scherf U, et al. *Synth Met* 1994;67(1–3):181–5.
- [30] Braig T, Müller DC, Gross M, Meerholz K, Nuyken O. *Macromol Rapid Commun* 2000;21(9):583–9.
- [31] Zhang YD, Hreha RD, Jabbour GE, Kippelen B, Peyghambarian N, Marder SR. *J Mater Chem* 2002;12(6):1703–8.
- [32] Bayerl MS, Braig T, Nuyken O, Müller DC, Gross M, Meerholz K. *Macromol Rapid Commun* 1999;20(4):224–8.
- [33] Liu S, Jiang X, Ma H, Liu MS, Jen AKY. *Macromolecules* 2000;33(10):3514–7.
- [34] Jiang X, Liu S, Liu MS, Herguth P, Jen AKY, Fong H, et al. *Adv Funct Mater* 2002;12(11–12):745–51.
- [35] Bozano LD, Carter KR, Lee VY, Miller RD, Pietro RD, Scott JC. *J Appl Phys* 2003;94(5):3061–8.
- [36] Chou MY, Leung MK, Su YO, Chiang CL, Lin CC, Liu JH, et al. *Chem Mater* 2004;16(4):654–61.
- [37] Michelle S, Liu YH, Niu JW, Ka HL, Huang YF, Luo J, et al. *Macromolecules* 2008;41(24):9570–80.
- [38] Wong KT, Chien YY, Chen RT, Wang CF, Lin YT, Chiang HH, et al. *J Am Chem Soc* 2002;124(39):11576–7.
- [39] Wu CC, Liu TL, Hung WY, Lin YT, Wong KT, Chen RT, et al. *J Am Chem Soc* 2003;125(13):3710–1.
- [40] Schein LB. *Phys Rev B* 1977;15(2):1024–34.
- [41] Halik M, Klauk H, Zschieschang U, Schmid G, Ponomarenko S, Kirchmeyer S, et al. *Adv Mater* 2003;15(11):917–22.
- [42] Silinsh EA, Éapek V. *Organic molecular crystals*. New York: American Institute of Physics; 1994.
- [43] Gundlach DJ, Lin YY, Jackson TN, Schlom DG. *Appl Phys Lett* 1997;71(26):4556–73.
- [44] Gundlach DJ, Nichols JA, Zhou L, Jackson TN. *Appl Phys Lett* 2002;80(16):2925–7.
- [45] Thesen MW, Krueger H, Janietz S, Wedel A, Graf MJ. *J Polym Sci Part A Polym Chem* 2010;48(2):389–402.
- [46] He J, Liu H, Dai Y, Ou X, Wang J, Tao S, et al. *J Phys Chem C* 2009;113(16):6761–7.
- [47] Lin KR, Kuo CH, Kuo LC, Yang KH, Leung MK, Hsieh KH. *Eur Poly J* 2007;43(10):4279–88.
- [48] Randall D, Lee S, editors. *The polyurethanes book*. New York: Wiley; 2002.
- [49] Suresh KI, Kishanprasad VS. *Ind Eng Chem Res* 2005;44(13):4504–12.
- [50] Green RJ, Corneillie S, Davies J, Davies MC, Roberts CJ, Schacht E, et al. *Langmuir* 2000;16(6):2744–50.
- [51] Li Y, Kang W, Stoffer JO, Chu B. *Macromolecules* 1994;27(2):612–4.
- [52] Crenshaw BR, Weder C. *Macromolecules* 2006;39(26):9581–9.
- [53] Hasegawa M, Ikawa T, Tsuchimori M, Watanabe O, Kawata Y. *Macromolecules* 2001;34(21):7471–6.
- [54] Kuo CH, Peng KC, Kuo LC, Yang KH, Lee JH, Leung MK, et al. *Chem Mater* 2006;18(17):4121–9.
- [55] Ku CH, Kuo CH, Chen CY, Leung MK, Hsieh KH. *J Mater Chem* 2008;18(12):1296–301.
- [56] Lim H, Noh JY, Lee GH, Lee SE, Jeong H, Lee K, et al. *Thin Solid Films* 2000;363(1–2):152–5.
- [57] Jeong H, Zou D, Tsutsui T, Ha CS. *Thin Solid Films* 2000;363(1–2):279–81.
- [58] Sun M, Li J, Li B, Fu Y, Bo Z. *Macromolecules* 2005;38(7):2651–8.
- [59] Jungermann S, Riegel N, Müller D, Meerholz K, Nuyken O. *Macromolecules* 2006;39(26):8911–9.
- [60] Paul GK, Mwaura J, Argun AA, Taranckar P, Reynolds R. *Macromolecules* 2006;39(23):7789–92.
- [61] Ko CW, Tao YT, Lin JT, Thomas KRJ. *Chem Mater* 2002;14(1):357–61.
- [62] Baba A, Onishi K, Knoll W, Advincula RC. *J Phys Chem B* 2004;108(49):18949–55.
- [63] Liu Y, Liu MS, Jen AKY. *Acta Polym* 1999;50(2–3):105–8.
- [64] Morgan PW. *Macromolecules* 1970;3(5):536–44.
- [65] Chou CH, Shu CF. *Macromolecules* 2002;35(9):9673–7.
- [66] Liu W, Wang J, Qiu QH, Ji L, Wang CY, Zhang ML. *Pigment Resin Technol* 2008;37(1):9–15.
- [67] Lo J, Lee SN, Pearce EM. *J Appl Polym Sci* 1984;29(1):35–43.
- [68] Tang R, Tan Z, Li Y, Xi F. *Chem Mater* 2006;18(4):1053–61.
- [69] Liu MS, Jiang X, Liu S, Herguth P, Jen AKY. *Macromolecules* 2002;35(9):3532–8.